Composites Part B 270 (2024) 111131

Contents lists available at ScienceDirect

Composites Part B

journal homepage: www.elsevier.com/locate/compositesb

Degradation behavior and ageing mechanism of E-glass fiber reinforced epoxy resin composite pipes under accelerated thermal ageing conditions

Dandan Liao [a], Tan Gu [b], Jie Liu [b], Siwei Chen [b], Fei Zhao [b], Son Len [a], Jingjie Dou [a], Xiwen Qian [a], Jun Wang [a,*]

[a] School of Mechanical Engineering, Sichuan University, Chengdu, 610065, China
[b] Petro China Planning & Engineering Institute, Beijing, 100083, China

ARTICLE INFO

Keywords:
Glass fiber reinforced composite pipe
Hydrothermal aging
Thermal oxidative aging
Degradation behavior
Aging mechanism analysis

ABSTRACT

In this work, accelerated ageing experiments with circulating air and simulated oilfield water were carried out at 95 °C on aromatic amine-cured GFRP pipes used in oilfield environments, with effective ageing times of 5000 h and 3000 h respectively. The differences in ageing behavior and ageing mechanisms of the GFRP tubes at different times under the two conditions were then analyzed and discussed. The changes in the apparent morphology and microstructure of the samples after thermal ageing were first observed using optical microscopy and scanning electron microscopy, and the results demonstrated that the thermal oxygen environment triggered more drastic color changes and obvious oxidation layers. The resin matrix manifests a large number of nano-scale micropores and modest matrix shrinkage pores in the micron size range, this is accompanied by damage to the fiber cross-section. Hydrothermal ageing causes further dissolution of the surface resin and dissolution of the exposed fibers. ATR-FTIR analysis verifies the increase in C═O bonding of the ester group during thermal oxidation and the decreasing strength of the C–O–C and C–H bonds, while the behavior of ageing water absorption and glass fiber hydrolysis is illustrated by changes in the intensity of the –OH and Si–O characteristic bands. NMR hydrogen spectroscopy verified the formation of amides, methyl ethers and carboxylic acids in the thermal oxidation products of epoxy resins. Furthermore, the decay pattern of the circumferential tensile strength indicates that the hydrothermal environment has a more significant effect on the mechanical properties of GFRP pipes, which is attributed to the physical dissolution of the surface resin, significant hydrolytic damage to the surface exposed fibers, and the combined damage to the resin-fiber interfacial bonding by chloride ions in simulated oilfield water.

1. Introduction

Compared with traditional metal pipes, fiber reinforced composite pipes are widely used in many fields due to their high specific strength, good corrosion resistance, excellent durability, wear resistance, tensile properties, as well as good corrosion resistance and scale inhibition properties [1,2]. It has become an important way of transporting water and chemical raw materials, and the most economical means of transporting oil and gas over long distances [3,4]. Among numerous reinforcement materials, glass fiber has become an economical and commonly used choice due to its excellent mechanical and insulation properties, as well as its resistance to degradation [5]. Glass fiber reinforced (GFR) composites are also known for their light weight, resistance of corrosion and high pressure [6,7]. In recent years, glass fiber reinforced plastic (GFRP) pipe has gradually become an alternative material to traditional steel pipes in the oil and gas sector and is an important means of reducing corrosion and cost [8,9]. In this context, ensuring the long-term stable operation of GFRP pipes is essential to ensure production safety. Evaluating the integrity of aged GFRP pipelines, especially in harsh oil and gas environments such as high temperatures from oil and gas extraction, corrosive media and sour gases, and mechanical stresses from pipeline operation, is particularly important in the oil and gas industry. Therefore, the impact of thermal aging on the performance of fiber-reinforced composite pipes generated in service environments is also considered to be of great necessity.

In recent decades, most of the research related to FRP pipes are based on glass fiber reinforced laminates or epoxy resin matrix, mostly focusing on the study of the effect of natural ageing on mechanical

* Corresponding author.
E-mail addresses: 1401939517@qq.com (D. Liao), srwangjun@scu.edu.cn (J. Wang).

https://doi.org/10.1016/j.compositesb.2023.111131
Received 8 May 2023; Received in revised form 5 December 2023; Accepted 7 December 2023
Available online 16 December 2023

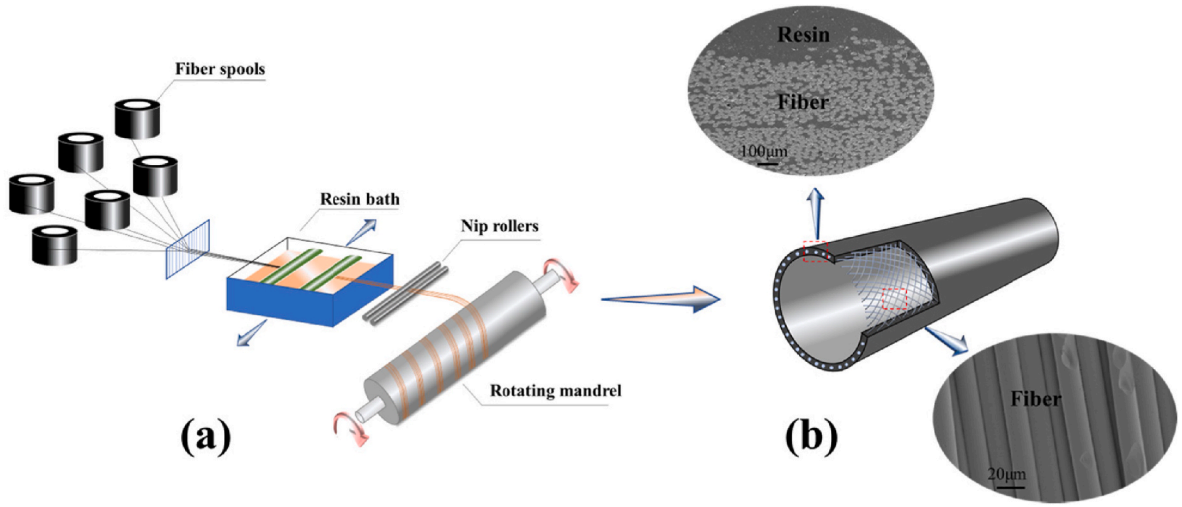

Fig. 1. Schematic diagram of (a) continuous winding process and (b) pipeline structure for glass fiber composite pipes.

properties under single factors. The effects of water immersion and hygrothermal ageing on the Mechanical behavior of fiber-reinforced epoxy composites have been extensively reported in the literature. Relevant works have shown that the effect of hydrothermal aging on glass fiber reinforced composite pipes is first manifested as damage to the fiber matrix interface [10,11], and then as the attenuation of macro mechanical properties such as interlaminar shear strength [12,13], tensile strength [14,15], bursting strength [16] and impact performance. Stocchi [17] reported changes in the mechanical properties of acid anhydride cured FRP tubes after 14 days of ageing in distilled water at 20 °C and 80 °C, ageing was observed to produce irreversible fiber matrix damage at the high temperatures, resulting in reduced flexural and impact properties. Reis [18] investigated the effect of ageing on failure pressure by subjecting GFRP tubes to hydrostatic tests at constant temperature (80 °C) and high pressure (1Mpa) for 6 months. It was found that the stiffness of tensile specimens was not significantly affected by the ageing time, but the ultimate tensile stress (UTS) was affected by the ageing time. Furthermore, studies on different humidity environments [19,20] and under different media conditions [21–23] have shown that high temperatures accelerate the diffusion and penetration of liquid phase media and have a significant reduction in the residual strength of fiber reinforced composites [24]. Similarly, the effects of thermal and photochemical ageing on the properties of fiber-reinforced composites show a consistent pattern, causing degradation and oxidation of the polymer backbone [25,26]. Some researchers have found that after thermal oxygen aging, the matrix and fiber/matrix interface in composite materials gradually deteriorate in the form of chain breakage [27], weight loss [28], and fiber/matrix debonding [29,30]. However, the degradation and decay of the epoxy resin is delayed by the action of fibers or other reinforcing phases [31]. Lafarie-Frenot [32–35] systematically investigated damage to epoxy laminates by thermal cycling in neutral and oxidizing atmospheres and found that the accelerating effect of oxygen and the coupling of thermal cycling had an accelerating effect on microcrack extension. Yang [36] investigated the thermo-oxidative ageing behavior of anhydride-cured epoxy resins at 130 °C and 160 °C. The results manifested a significant reduction in the free volume of the sample surface and a significant decrease in fracture strain and flexural strength. This is also a typical sign of thermal ageing behavior, where the composite as a whole is more dependent on the matrix and therefore more sensitive to thermal ageing factors. There are numerous studies on the aging of GFRP composite materials, but few studies have compared the aging behavior in a multi factor coupled environment. They focus on the surface changes in mechanical properties and mechanical behavior after aging. At the same time, there is little consideration given to the essential relationship between factors such as microstructure and chemical composition after aging and performance degradation during the aging process, and the research and discussion on the mechanism of thermal aging are not in-depth enough. At present, there is not a unified understanding of the aging and degradation mechanism of GFRP composite materials under the influence of multiple factors. However, the diversity of methods and the wide range of values also imply that further investigation deserves to be conducted before reaching a consensus on such a scientifically reasonable and feasible method in engineering.

In order to solve the aging failure problem of non-metallic composite pipes represented by glass fiber reinforced plastic (GFRP) in the oil and gas field environment, an experimental program based on the principle of time-temperature equivalence is designed in this work. Accelerated aging experiments were carried out on GFRP tubes in simulated oilfield produced water medium heated by hot air in a circulating hot oven and a constant temperature water bath. Using a combination of macroscopic experimental data and microstructural analysis, the aging behaviors of GFRP tubes with different aging times under the two environments were compared in terms of the microscopic morphology and organization, chemical and mechanical properties of the GFRP samples before and after aging, and the differences in the aging mechanisms were investigated. The oxidation behavior of the samples and the morphological and structural changes after aging were observed by optical microscope and scanning electron microscope; the compositional changes of the aging samples were determined by FTIR and NRM; the attenuation of axial and circumferential tensile strengths and modulus was evaluated by tensile method, and the failure mechanism of GFRP pipes under the influence of the main factors of the oilfield working conditions was analyzed. Meanwhile, in the next step, we plan to carry out the research on the aging mechanism and remaining life prediction method of FRP pipes under oil medium and stress environment. On the premise of clarifying the failure mechanism, we will establish a prediction model for the remaining life of FRP pipes in service environment, which can make timely risk assessment and prediction for the pipes in the field. This is of practical value to ensure the safe production in the field and of great significance to guarantee the stable operation of pipelines in the field.

2. Experimental

2.1. Materials and specimens

This work adopts the glass fiber reinforced pipes produced by Shandong Shengli Xinda Industrial Co., Ltd. whose structure contains an epoxy resin matrix as the bonding phase and glass fibers as the reinforcing phase. The pipe is prepared by a continuous winding forming

Table 1
Simulations composition of produced water from the Oilfield (Ionic content units/mg·L^{-1}).

Ionic species	Ca^{2+}	Mg^{2+}	SO_4^{2-}	HCO_3^-	Cl^-	Fe^{2+}	Na^+/K^+	pH
Concentration	6300	290	635	325	85,000	20	5000	5.7

process, using surface-treated glass fiber bundles as the reinforcing phase, which are uniformly infiltrated with resin glue and wound continuously around the mould core or liner at a certain winding angle (±45°), and then cured and demoulded to become a FRP pipe. The production process and pipeline structure of the pipeline are shown in Fig. 1. The glass fibers used in this line are commercial E glass fiber bundles (Owens Corning, 111A silane sizing, 300 tex), with a yarn width of 0.5 mm, a nominal diameter of 15 μm and a raw wire density of 300 tex. The resin solution used is based on Diglycidyl Ether of Bisphenol A (DGEBA) and contains the curing agent 4,4′ Diamino Diphenyl Methane (4,4′ DDM) and is cured by an internal heating process following a step-by-step procedure of 90 °C for 2 h, 110 °C for 1 h and 130 °C for 4 h.

2.2. Isothermal accelerated thermal aging

The GFRP pipe used in the experiments has an inner diameter of 76 mm and an outer diameter of 84 mm, with a pressure resistance of 5.5 Mpa. The accelerated thermal ageing consisted of both thermal oxygen ageing and hydrothermal ageing. The pipes were cut into 100 mm and 500 mm long sections, cleaned and dried, and then used for the thermal oxygen and hydrothermal tests respectively, with three control specimens in each group to ensure the accuracy of the experimental data. Based on the on-site investigation of the oil field site before the experiment, it was confirmed that the maximum operating temperature of the water injection pipeline at the site was lower than 65 °C, and in order to conduct the accelerated aging experiment it was necessary to appropriately increase the simulation temperature. The design of the experimental temperature is based on the high-temperature accelerated test procedure and the time-temperature equivalence principle in the standard API 15S, while taking into account the glass transition temperature of the epoxy resin matrix in the GFRP pipeline. The experiment was carried out with a maximum operating temperature increase of 30 °C (that is 95 °C) as the aging temperature, which is intended to accelerate the diffusion process but not to lead to premature degradation or to affect the degradation mechanism of the material. The field study also identified the composition of the field produced water and used this as the basis for configuring the produced water simulation solution for the laboratory environment, as manifested in Table 1 thermal oxygen ageing experiments were completed in an air circulation oven at 95 °C, which provided a continuous replenishment of oxygen in the ambient air. Hydrothermal ageing was carried out in a 95 °C water bath containing a simulated solution of oilfield produced water, with the solution volume determined to be 150 L in accordance with standard GB/T 1462–2005 ensuring a solution loading ratio greater than or equal to 8 mL/cm^2. The thermal oxygen ageing and hydrothermal ageing were carried out for 5000 h and 3000 h respectively. The samples were observed and weighed during the experiment and the pH of the simulated solution was adjusted with hydrochloric acid in time.

2.3. Characterization method

In order to further analyze the structural evolution of the aging samples in detail, the samples need to be cut and then polished with sandpaper, followed by optical microscopy to observe the appearance morphology and color changes of the GFRP tubes under different aging conditions, and to compare the growth of the oxide layer on the cross-section of the tubes. The microscopic morphology and structural characteristics of the fiber composite pipes were observed with a scanning electron microscope (ZEISS mini 300), the trend of increasing pores and resin defects on the inner and outer surfaces of the pipes after ageing was analyzed, and the damage at the fiber resin interface after thermal ageing was verified with a transmission electron microscope (FEI talos

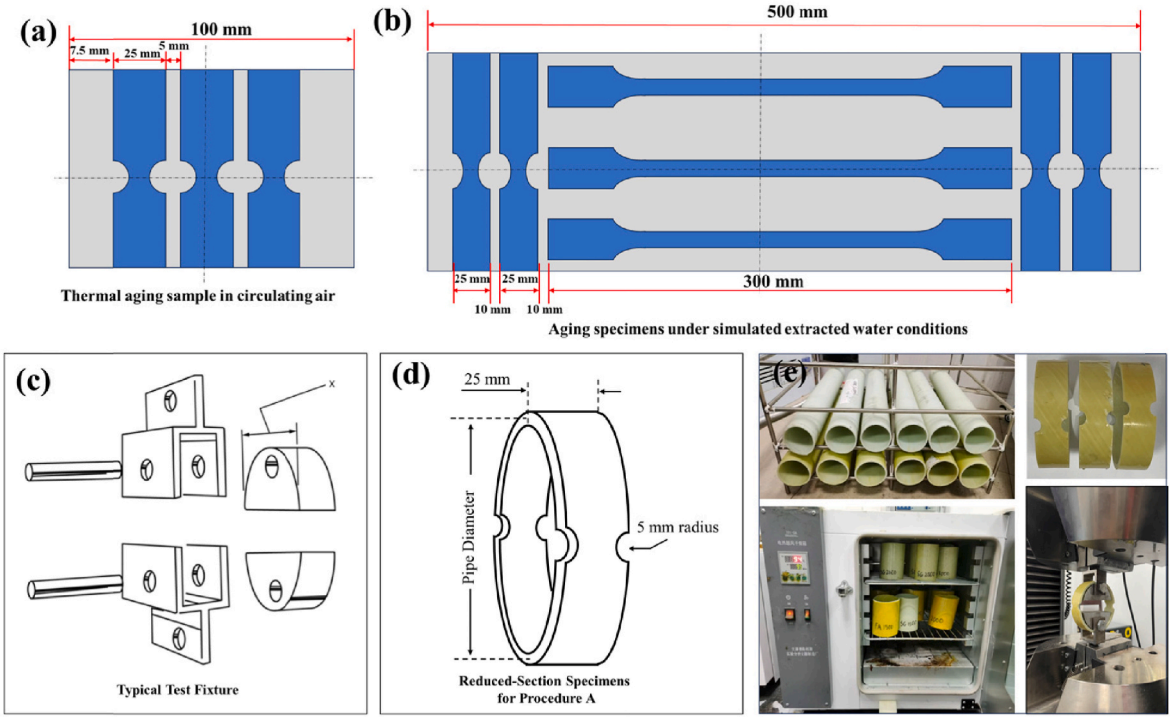

Fig. 2. Sampling schematic and testing procedure for hoop tensile strength testing by separating disk method.

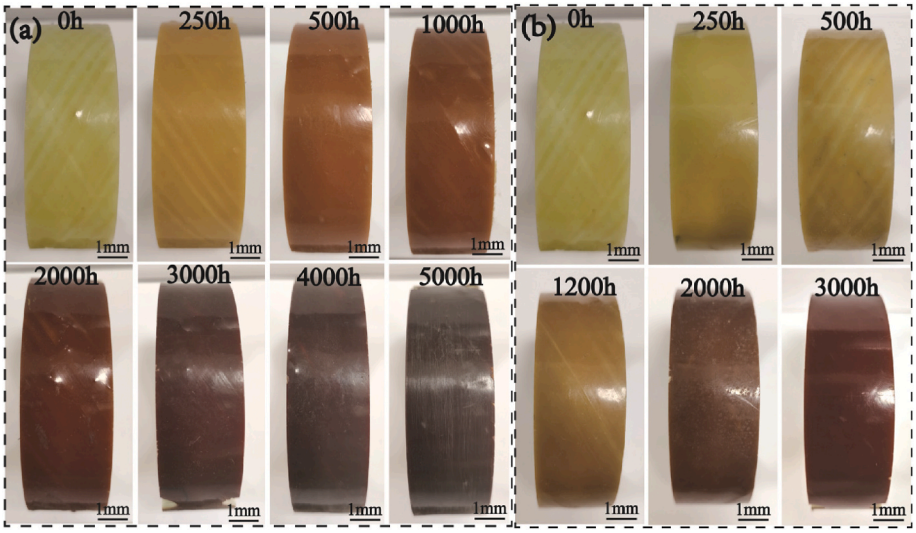

Fig. 3. Macroscopic surface morphology of (a) thermal oxygen aging for 5000h and (b) hydrothermal aging for 3000h.

F200× G2). In addition, for subsequent analysis of degradation behavior during thermal oxidation and hygroscopic behavior during hydrothermal aging, the overall weight of the sample before and after thermal aging needs to be weighed. The change in sample weight due to hydrothermal aging was recorded as a function of time as hygroscopicity, calculated by Equation (1) [37,38].

$$M_t = 100 \times \frac{W_t - W_0}{W_0} \tag{1}$$

Where M_t is the percentage moisture content of the specimen at time t (expressed as a function of the square root of the aging time), W_0 is the original weight of the specimen in the dry state, and W_t is the weight of the specimen at moment t.

For infrared spectroscopic testing, a cross-section of the sample was powdered with a file, mixed with potassium bromide, then ground thoroughly and pressed for testing. The changes in the chemical structure of the aged sample surface were investigated by Fourier transform infrared spectroscopy (FTIR, Nicolet 6700, Thermo Scientific) in the attenuated total reflection (ATR) mode in the range 4000–450 cm^{-1} with a resolution of 4 cm^{-1}. During the aging process, the thermal oxidation reaction introduces a large number of oxygen-containing groups such as (C–O–C, C═O, etc.) into the main chain of the epoxy resin, and the degree of oxidation is quantitatively characterized by the hydroxyl index in order to facilitate the analysis and comparison. The aging index represents the overall degree of oxidation by three indexes I (912 cm^{-1}), I (1224 cm^{-1}) and I (1738 cm^{-1}), which are used to represent the relative content C–O–C (846-969 cm^{-1}), C–O (1197-1274 cm-1) and C═O (1670-1760 cm^{-1}) bonding in the epoxy matrix, respectively. The formula is the ratio of the integral area of the corresponding band to the area of the reference methyl band (2580-2930 cm^{-1}, denoted as $A_{2580\text{-}2930\ cm\text{-}1}$, which remains constant during aging) [39], for example the aging index for carbonyl (C═O) is calculated as follows.

$$\text{Aging index } (I_{1738cm\text{-}1}) = \frac{A_{1670-1760cm^{-1}}}{A_{2580-2930cm^{-1}}} \times 100\% \tag{2}$$

where $A_{1670\text{-}1760\ cm\text{-}1}$ and $A_{2580\text{-}2930\ cm\text{-}1}$ denote the integral areas of the carbonyl band and the reference methyl band, respectively, and the samples under each condition were tested three times to ensure the reproducibility of the data. The ^{1}HNMR spectra were recorded at room temperature using Bruker Avance II-600 MHz NMR using deuterated chloroform ($CDCl_3$), as solvent and tetramethylsilane (TMS) as internal standard.

2.4. Mechanical tests

In the accelerated aging section, the GFRP tubes were cut into 100 mm sections for thermal aging under circulating air conditions. Due to the limitation of the sample size by the aging equipment, the aging specimens under this condition were only subjected to the tensile test of the split disk method according to ASTM D2290 for the hoop strength test, and the pipe segments were sampled as shown in Fig. 2a. The pipe section with a cut length of 500 mm was used for thermal aging in the extracted water environment, and both annular and axial strength tensile were carried out after aging. In addition to the annular strength characterization, the axial tensile properties of the fiber-reinforced thermoset plastic pipe were also determined according to the standard GB/T 5349–2005, and the sample was taken as shown in Fig. 2b. Ring tensile strength experimental method used in this experimental study is strictly based on procedure A in the standard ASTM D2290-12, which is applicable to the determination of the apparent tensile strength of reinforced thermosetting resin tubes. The experiments were carried out by the separating disk method, in which the fixture style used is shown in Fig. 2c and the specimen size specification is shown in Fig. 2d. The minimum width of the specimen was taken as 25 mm, the minimum width of the notched part was taken as 10 mm, and the two notches were distributed symmetrically at 180°. The experimental process is shown in Fig. 2e. The experimental parameters were selected according to the standard with the ambient temperature of 23 °C and the tensile rate of 10 mm/min in the tensile process.

The ultimate breaking load was measured experimentally and then the circumferential tensile strength of the GFRP pipe was calculated according to Eq. (3).

$$\sigma_{a=} P_b / 2A_m \tag{3}$$

Where σ_α is the apparent yield or ultimate tensile stress of the specimen, (MPa); P_b represents maximum or breaking load, or both, (N); and A_m is the minimum cross-sectional area of the two measurements, mm^2.

3. Results and discussion

3.1. The effect of thermal aging on macrostructure and microscopic morphology

Fig. 3 demonstrates the color and appearance changes of aromatic

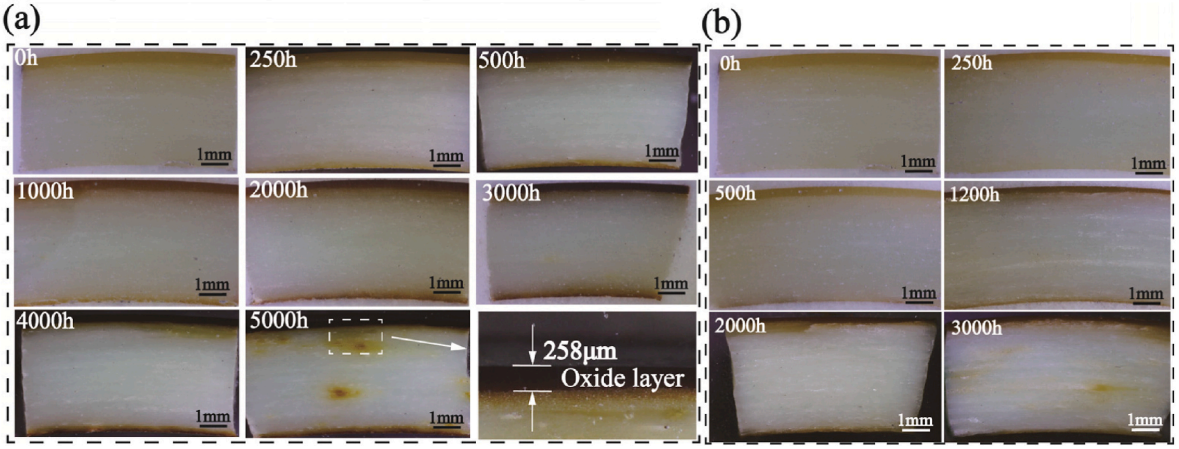

Fig. 4. Macroscopic cross-sectional morphology of samples (a) thermal-oxygen aging for 5000h and (b) hydrothermal aging for 3000h.

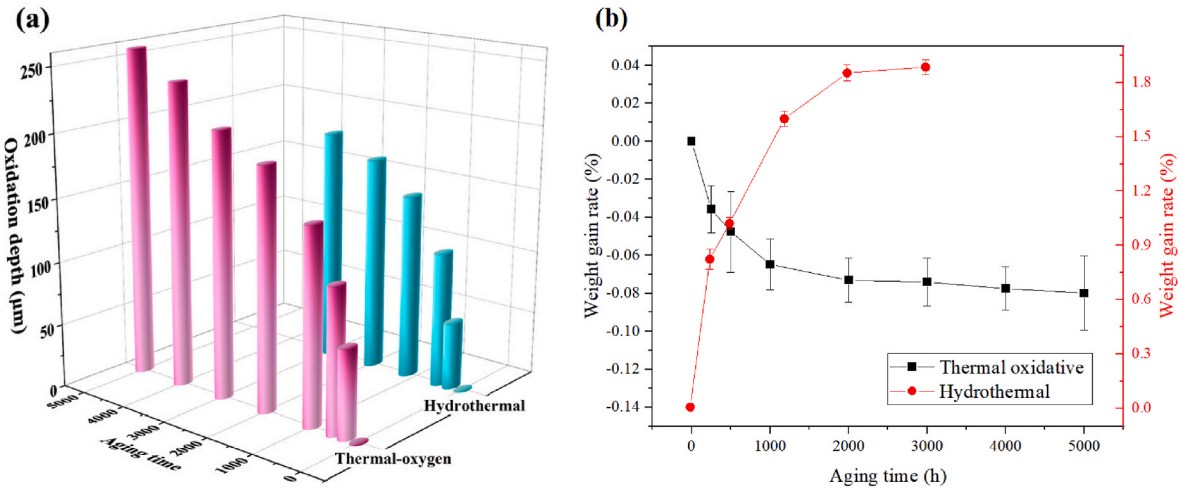

Fig. 5. Physical properties of GFRP tubes after thermal aging at 95 °C under two conditions (a) aging time vs. oxidation depth curve, (b) aging time vs. weight gain curve.

amine cured GFRP pipes after aging for different times under 95 °C thermal oxidation environment. The results showed that the GFRP pipes in the initial state manifested chartreuse, and the color gradually deepened with the aging time. The color of outer layer changed from chartreuse to brown after 1000 h of oxidation, and then further transformed to black after 5000 h. The color change indicates that the epoxy resin undergoes a chemical reaction due to thermal oxidation [40], related studies have demonstrated that the deepening of the color of epoxy resins after thermal aging may be related to the formation of polyolefin structures and the synthesis of quinone or cyclized conjugated nitrogen compounds [26]. There are literature also reports that color changes are related to the invasion of oxidative degradation products [41]. From Fig. 4a, it can be observed that the changes in the oxide layer on the cross-section of GFRP tubes after thermal aging, oxidative degradation occurs first in the exposed areas of the surface. The oxidation layer also darkens with increasing aging time and the oxidation depth further increases. In comparison, Fig. 4b manifests that the surface color of the hydrothermal ageing samples is lighter than that of the thermal oxygen ageing samples at the same ageing time, but obvious signs of water absorption are also found in the core of the sample.

Related research [40,42] has demonstrated that the resin layer that changes color significantly after thermal ageing can be defined as the surface oxide layer, and the oxidation depth can be counted and then the damage depth can be calculated. The oxidation depth of the aged specimens was counted according to the above method and the results are shown in Fig. 5a. The results indicate that the oxidation depth rapidly increases in the early stage of aging, and the growth rate slows down and tends to stabilize in the later stage. The oxidation depth reaches 183.7 μm after 3000 h of hydrothermal ageing, the depth of the oxidation layer reached 208.5 μm after 3000 h, and after 5000 h, it was 258 μm. Due to the differences in the internal and external structures of the pipes, the resin rich layer on the outer surface is pure epoxy resin, which rapidly oxidizes under the action of oxygen and high temperature. The reinforcement effect of glass fibers inside the pipeline makes it difficult for the medium to diffuse and hinders the oxidation process [42]. The core is protected by both the inner and outer layers and is not oxidized, but a damaged area of the core was also observed after 5000 h. This phenomenon indicates that the oxygen medium has diffused to the core of the material after prolonged aging. The large number of micropores generated inside the aged composite material provide channels for the permeation and diffusion of oxygen, while the high temperature of the environment accelerates the diffusion of oxygen into the material. The hygroscopicity results of thermally aged GFRP tubes are shown in Fig. 5b, which shows the variation of water content with aging time.

The weight change curves in both thermo-oxidative and hydrothermal environments can be divided into two phases, showing rapid changes at the beginning of the aging period and a steady slow growth subsequently. In the thermal oxidation process due to oxidative degradation of the epoxy resin leads to breakage of the main chain molecules into small molecules, and weight loss is the main feature in this process.

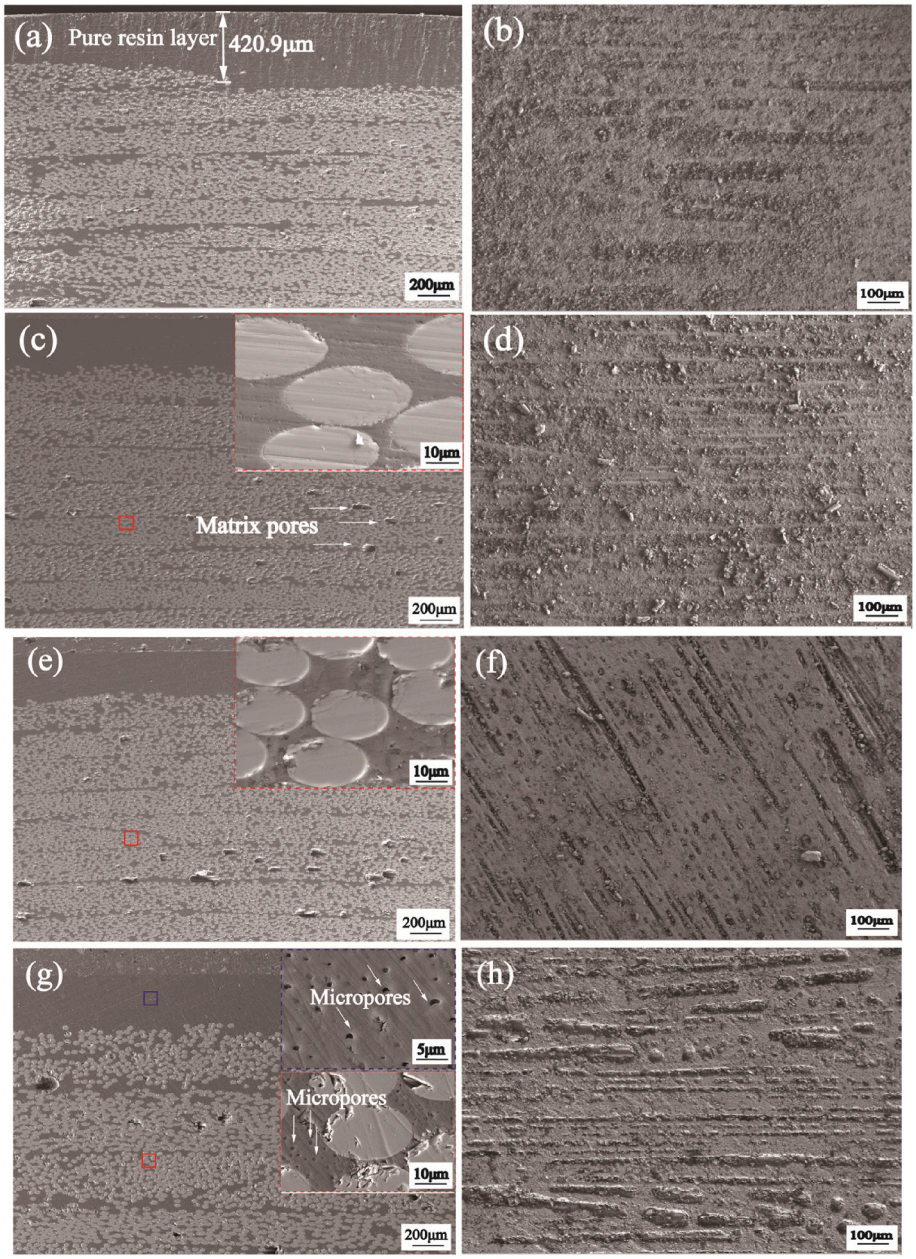

Fig. 6. Microscopic cross-sectional morphology (a) 0h, (c) 500h, (e) 3000h, (g) 5000h and internal surface morphology (b) 0h, (d) 500h, (f) 3000h, (h) 5000h of thermal oxygen aging at 95 °C.

In the first stage of thermal oxidation, the continuous heat input accelerates the oxidative degradation of the resin molecules, resulting in the formation of small molecule products and leaving dense pores in the pipe cross-section. This phenomenon was observed in scanning electron microscopy images of the pipe cross-section. In the second stage of thermal oxidation, prolonged heat leads to post-curing of the epoxy resin and an increase in resin cross-link density, which makes the matrix structure more stable and slows down the rate of oxidative degradation of the resin. During hydrothermal aging, the absorption of water by the GFRP pipe competes with the decomposition of the resin due to high temperatures. In the first stage of hydrothermal aging, the sharply increasing slope implies a rapid moisture absorption process in the specimen, which can be well predicted by the fickian model [37,43]. At this point, the effect of hygroscopic behavior dominates and is manifested by a continuous increase in overall weight. In the final stage of hydrothermal aging, a continuous hygroscopic process leads to a slowing down of water absorption until a moisture saturation level is reached, and it has been shown that both prolonged immersion and supersaturated moisture absorption adversely affect the mechanical properties of glass fiber/epoxy composites [44].

The asymptotic micromorphology of the specimens at different aging times is shown in Fig. 6. The cross-section shows that in the initial state there is a pure resin layer with an average thickness of approximately 420 μm, which is dense but not uniform (in Fig. 6a). The single glass fiber in the cross-section is 15 μm in diameter and the fiber is tightly bound to the resin interface but not uniformly distributed between the layers. Fig. 6b demonstrates the morphological characteristics of the inner surface of the pipe, which shows a few linear pits on the inner wall of the pipe caused by insufficient resin filling.

As the thermal oxidative ageing process continued, distinct matrix holes were observed in the cross section of the GFRP pipe after 500h (Fig. 6c). The resin on the inner surface of the pipe underwent significant shrinkage and deformation, and the fibers showed signs of gradual exposure. Lafarie-Frenot found similar matrix shrinkage holes in epoxy

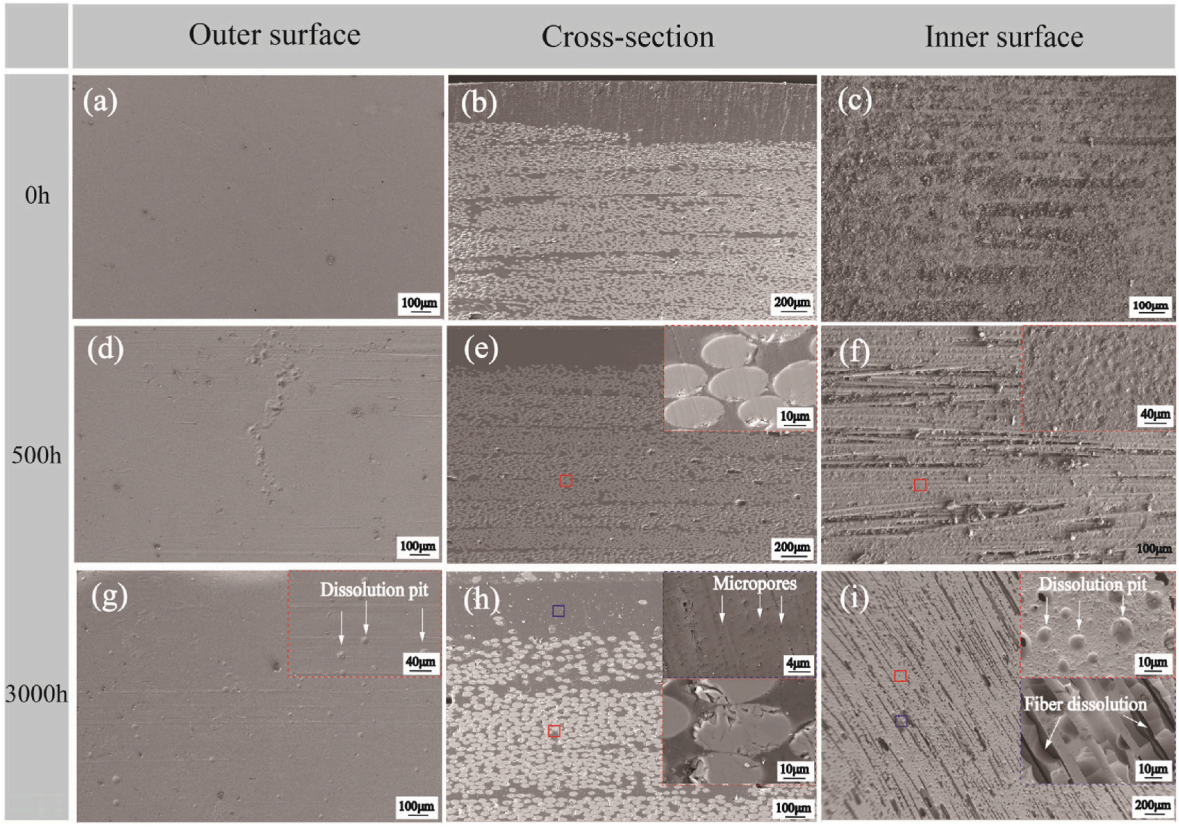

Fig. 7. Effect of 95 °C hydrothermal aging on the appearance and morphology of GFRP tubes.

resin sheets in thermal cycling ageing experiments and attributed the cause to the presence of high local stresses in the matrix and fibers leading to interfacial cracking and shrinkage [34]. Yang [45–47] et al. systematically investigated the thermal oxidation behavior of fiber-reinforced ceramic matrix composites with a two-dimensional woven structure under different conditions, and demonstrated a direct correlation between the porosity and the changes in the mechanical properties of the composites after aging. After 3000 h of ageing, a significant increase in the number of fiber exfoliation holes can be observed in the cross-section of the pipe, the epoxy resin matrix between the fibers starts to manifest significant microporosity (Fig. 6g). The inner surface resin demonstrates significant exfoliation, forming significant linear defects leading to partial exposure of the fibers to the oxygen environment. After the final 5000 h ageing experiment, a large number of micro-pores were found on both the pure resin layer on the surface and the resin between the glass fibers, with a maximum size close to 500 nm. The glass fiber interface also demonstrated severe damage, while the shrinkage of the resin on the inner surface became more pronounced.

It is found that the hydrothermal ageing process of GFRP tubes is accompanied by ageing characteristics similar to those of thermal oxygen ageing. Compared with thermal oxygen ageing, hydrothermal ageing differs in that it involves a complex combination of chemical reactions and physical dissolution processes [21]. Morphological analysis revealed that the damage to the fiber interface caused by hydrothermal environment was more severe than that caused by thermal and oxygen aging, as evidenced by the widespread fiber damage observed in Fig. 7i. The micro-pores and the matrix holes became increasingly evident as the degree of aging increases. In addition, a large number of uniformly distributed circular corrosion pits with a maximum diameter of 20 μm were observed on the inner and outer surfaces of the pipe after hydrothermal aging for 3000 h. These phenomena indicate that both the dissolution damage to the glass fiber and the corrosion pits on the resin surface are related to the hydrolysis process.

3.2. Analysis of the chemical composition

Fig. 8 manifests the IR spectrum of the FRP tube after thermal oxygen ageing. For comparison, the spectra were panned vertically so that their baselines overlapped and magnified in specific spectral bands. Observation of Fig. 8 a demonstrates that no new peaks appear in the IR spectrum after ageing and the spectrum is consistent with that of the unaged specimen, indicating that no decomposition of the material has occurred. Analysis of the bands revealed that the peaks at 3320 cm^{-1} and 1650 cm^{-1} are characteristic peaks for the N–H bonding in the amine chain in amine-cured epoxy resins [26]. Calibration and identification of the characteristic peaks showed that the peaks at 3500 cm^{-1} were the stretching vibrations of O–H bonds, 3050 cm^{-1} were benzene ring-H bonds, 2580-2930 cm^{-1} were C–H and CH_2, 1580-1610 cm^{-1} were aromatic ring signals, and 1460 cm^{-1} were absorption peaks of stretching vibrations of CH_2 bonds. Comparison of the changes in peak intensity between the different spectral bands reveals that the broad band increases and the peak position shifts between 3200 cm^{-1} and 3600 cm^{-1} after ageing, and that the spectral band is probably a tension signal of the hydroxyl group, which is a result of the overlap of the spectral bands characteristic of the epoxide anhydride reaction and many oxidation products [29]. Some researchers have demonstrated that C═O and C–O–C are the main functional groups in the volatile products of thermal degradation of resins [48]. Therefore, the degree of oxidation can be expressed by quantitative analysis [39] of the infrared spectrum through three ageing indices $I_{(912\ cm\text{-}1)}$, $I_{(1224\ cm\text{-}1)}$ and $I_{(1738\ cm\text{-}1)}$, which are used to represent the relative C–O–C at 846-969 cm^{-1}, C–O at 1197-1274 cm^{-1} and C═O bond at 1670-1760 cm^{-1} respectively which is defined as the ratio of the area of the C═O band (1670-1760 cm^{-1}) to the area of the reference methyl band (2580-2930 cm^{-1}, constant during ageing).

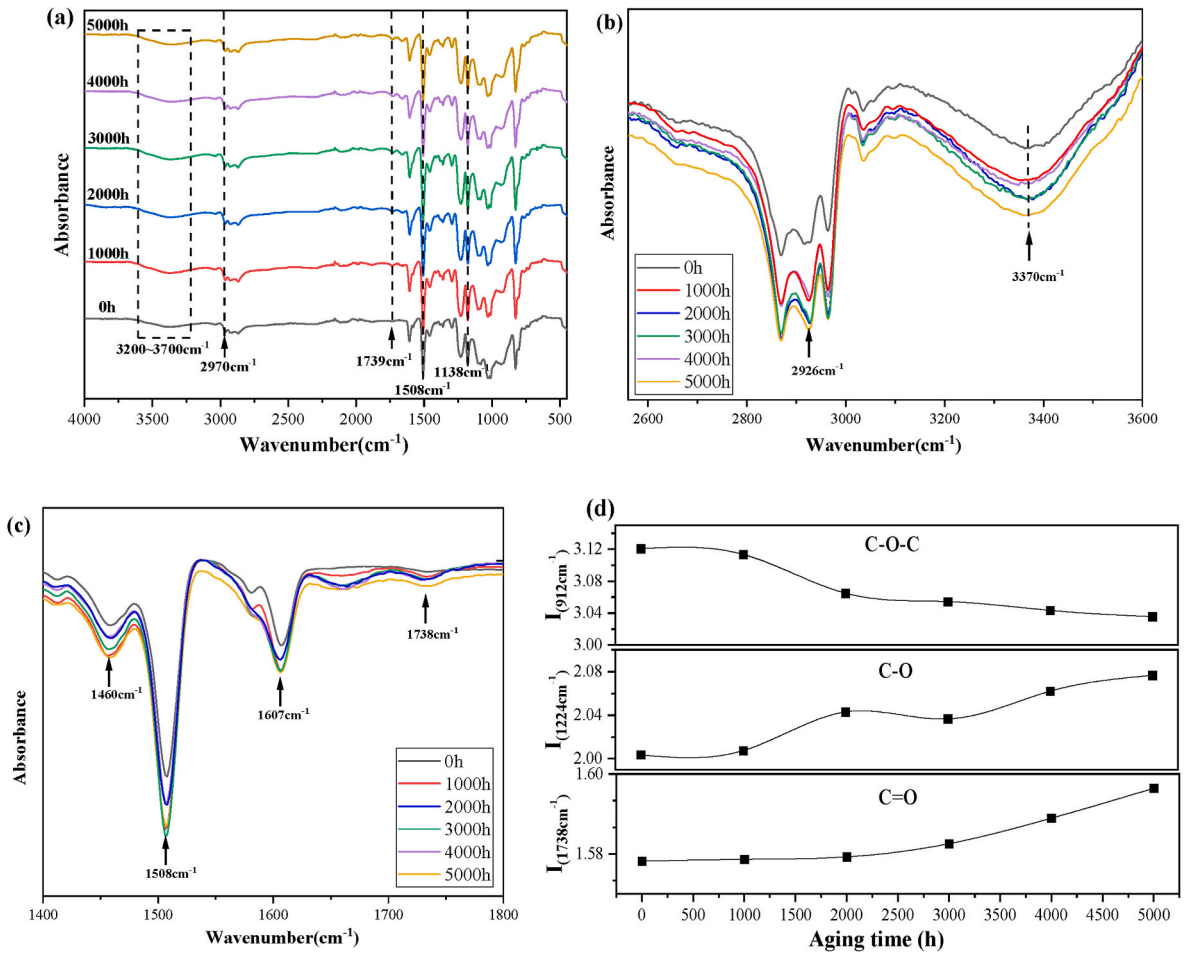

Fig. 8. Infrared spectra of samples aged at different thermal oxidation times (a) full spectrum, (b) (c) local magnification, (d) ageing index.

$$\text{Aging index } (I_{1738cm\text{-}1}) = \frac{A_{1670-1760cm^{-1}}}{A_{2580-2930cm^{-1}}} \times 100\%$$

Where $A_{1670\text{-}1760}$ and $A_{2580\text{-}2930}$ indicate the integral areas of the carbonyl and reference methyl bands respectively, samples were tested three times for each condition to ensure reproducibility of the data. It was found that as the signal of the C–O–C band decreased, an enhancement of the C–O at 1224 cm^{-1} and the C═O characteristic band at 1738 cm^{-1} was observed, and as the carbonyl and ether indices in the IR spectrum increased, the epoxide index decreased, indicating that oxidation of the epoxide group on the main chain had occurred. The intensity of the C–H characteristic bands around 958 cm^{-1}, 2923 cm^{-1} and 2854 cm^{-1} were also found to decay, these phenomena indicate that the C–H bond in the methyl or methylene group between the benzene rings is oxidized and the oxygen atom attacks the C–H bond attached to the hydroxyl group on the main chain to form an acid compound first, which continues to break to form small molecules of gas, as in the reaction equations (1) and (2). It is noted in the literature [49] that the ester group is more heat resistant than the ether group, and the molecular chain will break at the β position of the alcohol group, which will produce compounds containing esters, ketones and aldehydes. The curing agent will also continue to decompose under the action of oxygen after the bond break, and the N element in the curing agent connected to the epoxy resin will be oxidized to the C═O bond in the amide.

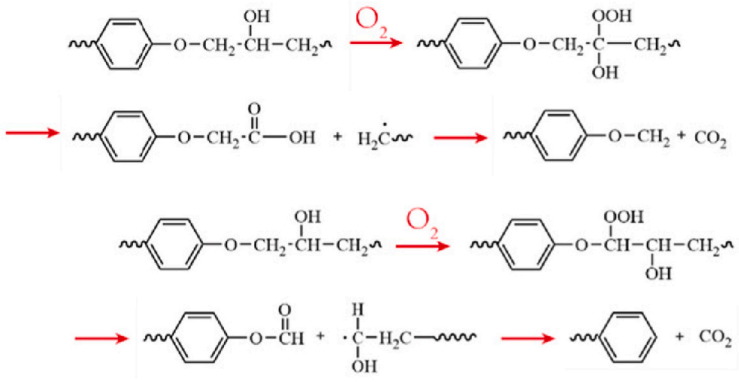

(1)

(2)

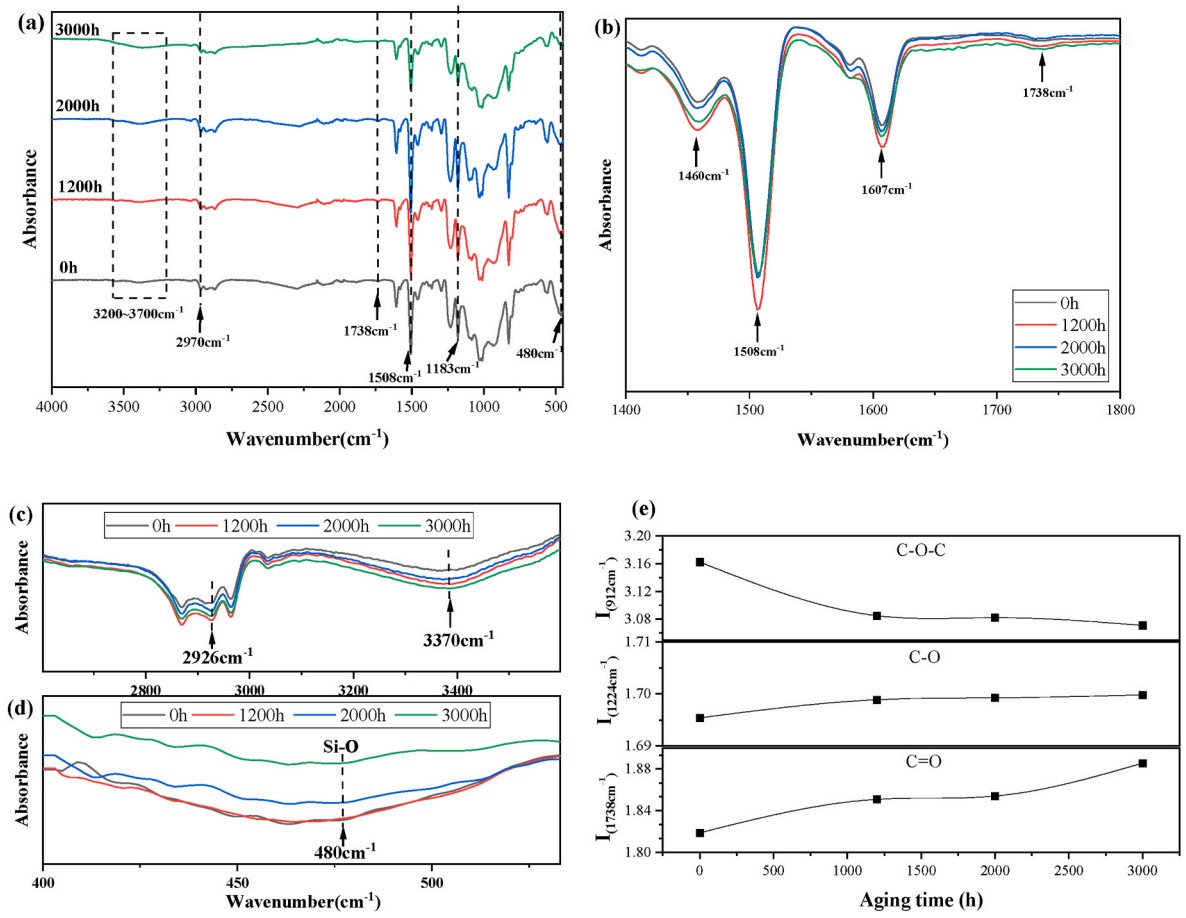

Fig. 9. Infrared spectra of samples after hydrothermal ageing at different times (a) full spectrum, (b) (c) (d) local magnification, (e) ageing index.

The changes in the chemical composition of the hydrothermally aged samples were characterized by infrared spectroscopy as shown in Fig. 9, detailing the functional groups of the main absorption peaks. Compared to the FTIR spectrum of the original GFRP, the intensity of the absorption peaks at spectra 1738 cm^{-1}, 1508 cm^{-1} and 1183 cm^{-1} increased slightly after ageing. These absorption peaks are associated with the C═O bond in the ester chain, the aromatic structure and the epoxy bond in the fatty ether group [50], respectively. The difference with thermal oxygen ageing is that a distinct peak is observed in hydrothermal ageing located at 3200-3700 cm^{-1}, which is caused by hydroxyl (-OH) stretching [51]. This phenomenon is related to the water absorption behavior of glass fiber reinforced plastics and Jojibabu [31] responded to the extent of water absorption by the intensity of this absorption peak. Based on this conclusion, we can find that the GFRP tube has the most severe absorption of water after hydrothermal aging for 3000 h. In addition, other researchers have found that the absorption peak at 480 cm^{-1} correlates with the Si–O bond in the glass fiber. In the present experiments it was also found that the intensity of the Si–O peak decayed significantly with increasing ageing time, which can be explained by the hydrolysis of the glass fiber during hydrothermal ageing [21,52,53]. The microstructure after hydrothermal aging in Fig. 7 also verified the morphology of the fibers after hydrolysis, and it has been shown in the literature that the process of glass fiber hydrolysis is related to the destruction of siloxane bonds in the glass by hydroxide ions, which further results in the gradual dissolution and destruction of the silicate network, and the formation of silicate that migrates into the solution [54–56].

^{1}H NMR was used to further characterize the structure of the epoxy resin matrix in its pristine state and to compare the changes in the structure of the resin after ageing, as shown in Fig. 10. The structures of the epoxy resin matrix in the initial state were found by comparison to include (^{1}H NMR, $CDCl_3$) δ (ppm): 7.14–6.8 (aromatic ring proton), 3.65 (CH_2OH), 2.05 (CH_3CO), 1.8–1.6 (CH_3), 1.25 (CH_3CH_2). After thermal-oxidative ageing the resin structure was altered and some significant new peaks were observed on the NMR hydrogen spectrum, no significant compositional changes were found after hydrothermal ageing. A comparison with the literature [57–59] confirmed the amide signal at 6.72 ppm, diglyme at 3.57 ppm and some signals for dimethoxyethane and carboxylic acids. This indicates that degradation of the resin composition occurred after oxidation, producing some new substances in agreement with the analytical results of the IR spectra.

3.3. The effect of thermal aging on mechanical behavior

In order to assess the ability of the GFRP tubes to withstand internal pressure, tensile stress-strain curves of the aged specimens were obtained by means of a circular tensile test. The tensile behavior of the thermally aged composite tubes at 95 °C is given in Fig. 11, which also shows the variation in tensile properties under different ageing conditions. The tensile behavior of the GFRP ring specimens was found to exhibit typical brittle fracture characteristics, with the tensile process progressing directly from elastic deformation to fracture without the presence of a plastic deformation stage and yielding stage. A slight increase in the tensile strength of the GFRP tubes was found to occur at 50 h of thermal oxygen ageing based on comparison of the tensile data, which may be related to the post-curing at the beginning of the ageing period. Also, the change in properties during thermal ageing is a result of the competing effects of post-curing induced thermo-oxidative degradation and matrix hardening [60]. A significant decrease in the tensile strength of the composite with increasing ageing time is observed in

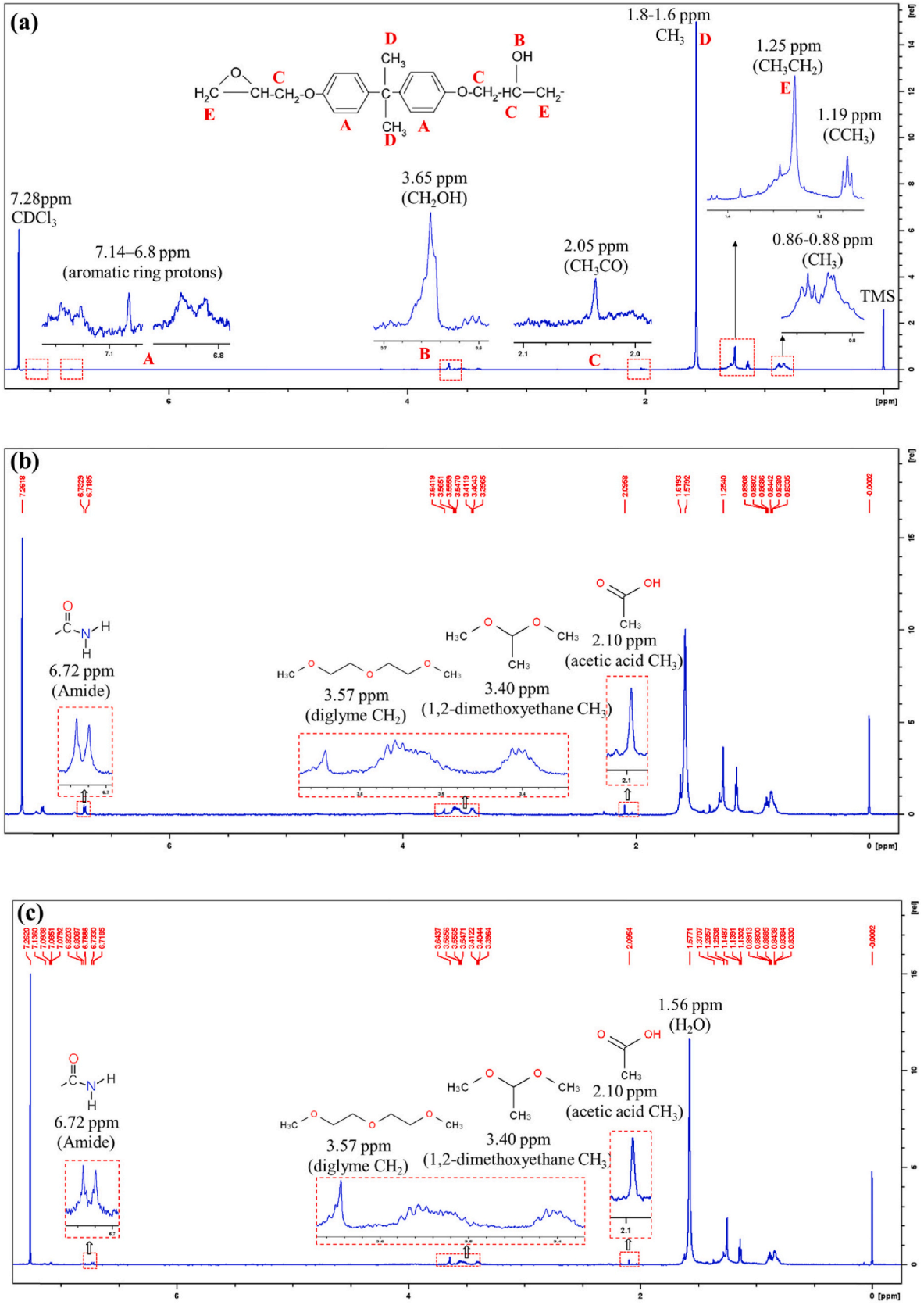

Fig. 10. ^{1}HNMR spectra of epoxy resin in FRP tubes after ageing (a) pristine, (b) thermal oxygen ageing for 5000h, (c) hydrothermal ageing for 3000h.

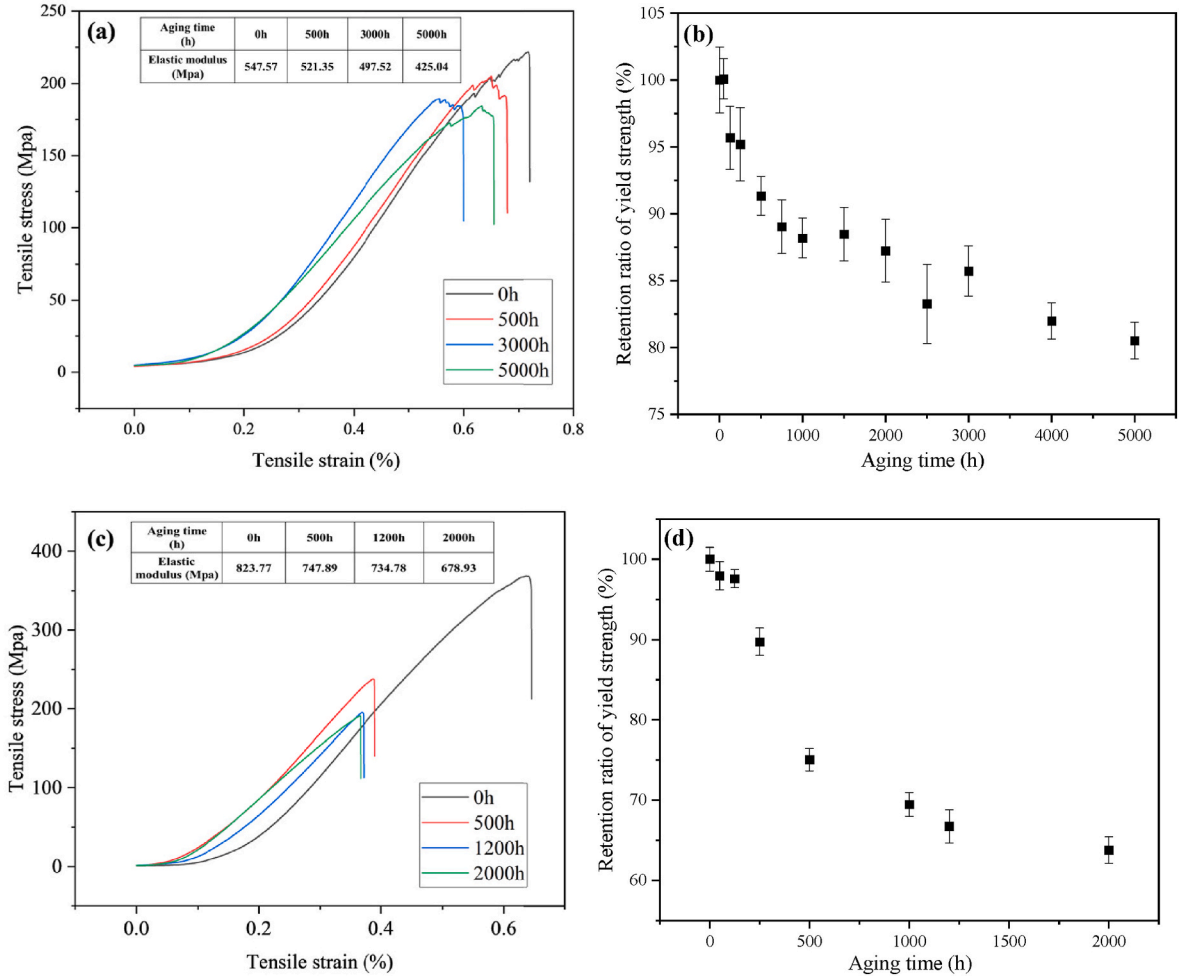

Fig. 11. Tensile curves and tensile strength retention of specimens after thermal ageing (a) (b) Thermal oxygen ageing, (c) (d) Hydrothermal ageing.

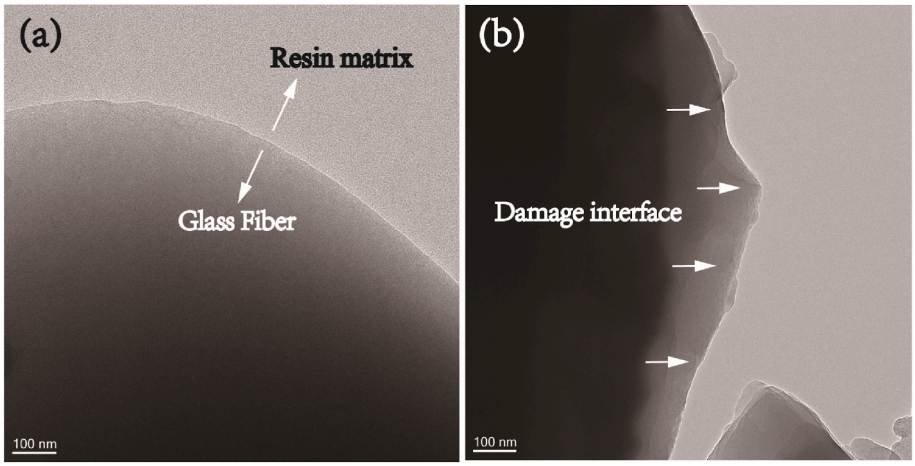

Fig. 12. TEM of the damaged area at the fiber-resin interface before and after thermal oxygen ageing (a) pristine, (b) after 5000h ageing.

Fig. 11 b. The initial slope increases significantly and plateaus after prolonged ageing. In comparison, the hydrothermal ageing samples demonstrated shorter ageing times, but more significant property degradation in terms of elastic modulus and tensile strength. This is explained by the fact that hydrothermal ageing causes the resin on the GFRP surface to physically dissolve and form corrosion pits, causing the exposed fibers on the surface to hydrolysis and form significant defects. The chloride ions in the simulated fluid prevent the formation of intramolecular and extra-molecular hydrogen bonds in the composite [61], causing damage to the bonding properties at the fiber/resin interface.

Fig. 12 demonstrates the damage to the microscopic interface of GFRP pipes following thermal and oxygen ageing, with significant damage to the resin fiber interface observed following thermal ageing.

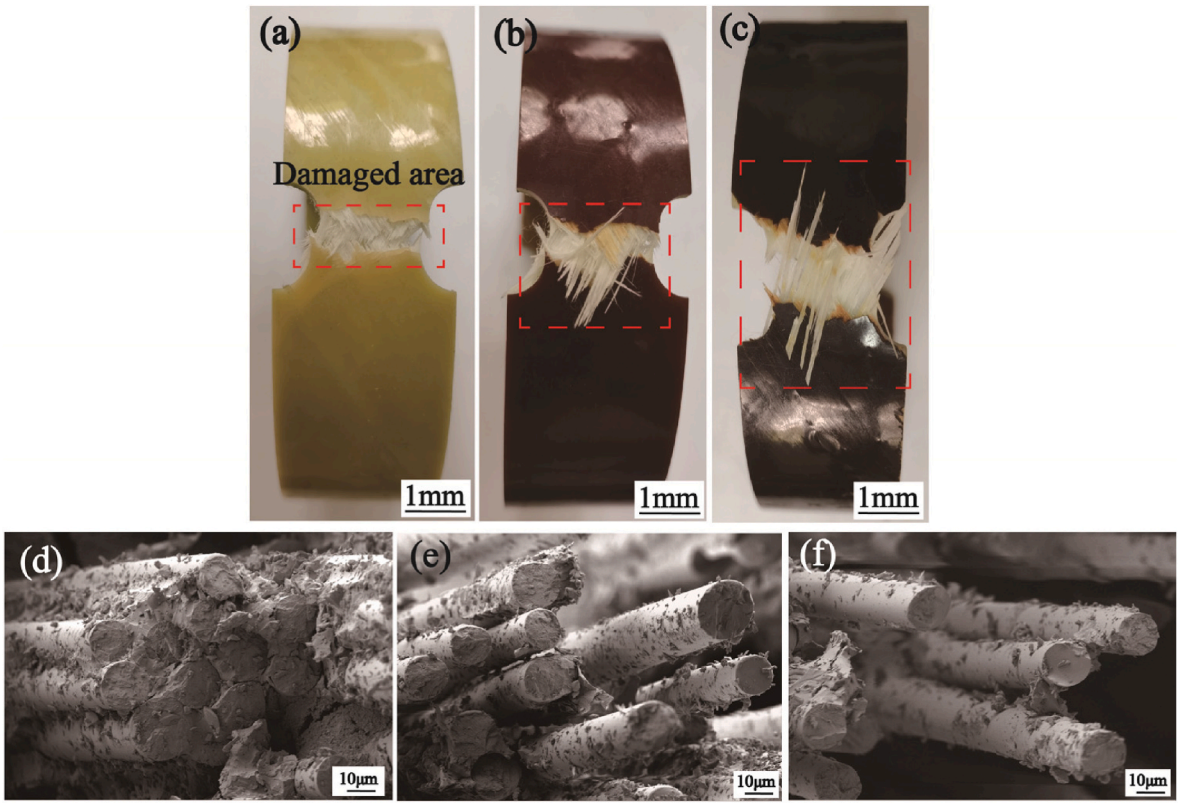

Fig. 13. Macrostructure of tensile fracture and microscopic morphology of fiber pull-out (a) (d) pristine, (b) (e) Sample for 3000 h by hydrothermal aging, (c) (f) Sample for 5000 h by thermal oxygen aging.

Fracture studies are essential to correlate the different failure mechanisms for each condition and outcome, where the main observation is the correlation between fiber pull-out and fiber/matrix interface quality and fiber bundle fracture. The fracture morphology of the tensile specimens after ageing was analyzed in Fig. 13, and it was compared the macroscopic fracture and microstructure of the samples after tensile fracture. From the macroscopic features of the fractures (Fig. 13a-c), it can be observed that the samples in the initial state have a neat fracture with a small damage area and inconspicuous fiber pull-out, while the damage deformation area is significantly larger and obvious fiber pull-out is observed in the aged specimens. It has been shown in the literature that the interfacial properties between the reinforcing fibers and the resin matrix can be quantified by using interfacial shear strength (IFSS) [62]. Observation of SEM images of fractured interfaces of fiber-reinforced epoxy resin materials revealed that some matrix particles adhered to the fiber surface after the structure of the fiber-reinforced composites was disrupted. The IFSS results suggest that stronger interfacial shear strength leads to an increase in epoxy resin on the fiber surface, and that better interfacial properties are manifested in better adhesion properties. The micromorphological features (Fig. 13d-f) shows that the fibers in the tensile fracture of the initial state samples are completely encapsulated by the resin. Fracture of the specimens showed complete fracture in the fiber bundles without fiber pull-out, which is evidence of good fiber/matrix bonding. Fiber debonding from the resin was observed in the fractures of both sets of samples after ageing and the fractured fibers had a long pull-out length. This can be explained by the fact that the action of oxygen and moisture directly affects the fiber/matrix interface, leading to a weakening of the bond and fiber pull-out. This further leads to a reduction in fracture toughness and a reduction in tensile strength.

3.4. Analysis of ageing mechanisms

The structural characteristics of the GFRP pipe in its original state are shown in Fig. 14a. The epoxy resin matrix has a crosslinked mesh physical structure, which contains a fully cured crystalline portion and an incompletely cured amorphous portion. The bonding between the resin matrix and the glass fibers is dominated by mechanical bonding and hydrogen bonding. The resin and fiber interfaces in the initial state of the pipe cross-section are well bonded without obvious defects. When high temperature and oxidizing atmosphere are introduced, the pipe aging rate increases. Due to the difference in thermal conductivity between the resin matrix and the glass fiber, the addition of high temperature causes thermal stress at the interface, resulting in shrinkage and deformation of the resin matrix and breakage of the fiber cross-section, as shown in Fig. 14b. The macroscopic morphology is characterized by a good bonding between the resin and the fiber in the initial state. The macroscopic morphology is characterized by resin shrinkage holes observed in the pipe cross-section, and some resin shrinkage is observed on the inner surface of the pipe resulting in fiber exposure. However, the pure resin structure on the outer surface of the pipe is uniform and dense, and the thermal stress generated by the additional high temperature is very small, so it does not trigger significant shrinkage and deformation in the pure resin layer.

In the early stage of thermal oxidation, the continuous heat intake accelerates the oxidative degradation of resin molecules. In the late stage of thermal oxidation, the prolonged heat leads to post-curing of the epoxy resin, which slows down the oxidative degradation of the resin. In our study, we found that after 500 h of thermo-oxidative aging, the resin matrix in the cross-section of the GFRP pipe began to show micropores formed by the escape of small molecule products. A large number of uniform nanoscale micropores were found in the resin matrix after 5000 h of aging (Fig. 6g) and compositional changes in the aged samples were detected by infrared. The molecular chain of the epoxy resin is degraded

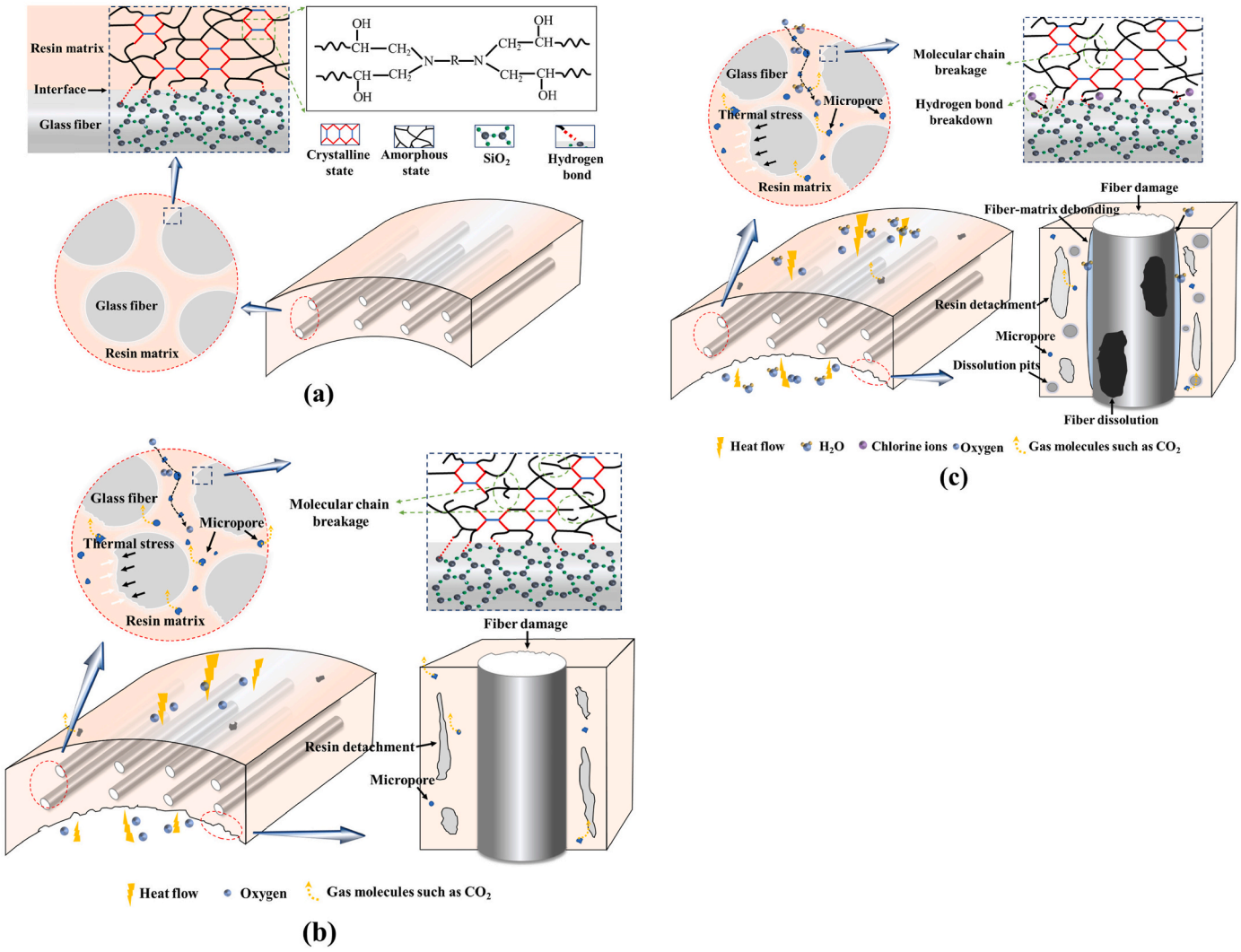

Fig. 14. Schematic diagram of the ageing mechanism of the two thermal ageing methods (a) pristine; (b) Thermal oxygen ageing; (c) Hydrothermal ageing.

under the continuous action of high temperature and oxygen, and it has been documented that the oxidative decomposition reaction of epoxy resins preferentially generates small molecules such as CO_2, CO, H_2O [27]. Further, oxidation of benzene ring hydrogen, methyl and methylene, and epoxy bonds on the main chain produces aldehydes, ketones, esters, or carboxylic acid products.

In comparison to thermo-oxidative aging, hydrothermal aging is differentiated in that the liquid phase medium further promotes the aging reaction. Moisture absorption and weight loss by degradation compete with each other in the aging process of GFRP pipes, but overall moisture absorption is more dominant, which is manifested in the continuous increase of overall weight. Hydrothermal aging promotes the dissolution of the resin on the inner and outer surfaces, forming a large number of dissolution pits and interfacial damage in the surface layer of the pipe, as shown in Fig. 14c. The GFRP pipe is then subjected to the process of hydrothermal aging. In turn, the creation of defects accelerates the moisture absorption process of GFRP pipes. In addition, the action of water molecules will promote the hydrolysis of glass fibers, and chloride ions in the simulated solution will hinder the formation of intramolecular and extramolecular hydrogen bonds in the composites, resulting in the degradation of the adhesive properties of fibers and matrix. All of these would adversely affect the mechanical properties of the glass fiber/epoxy composites. We also observed resin dissolution pits and severe glass fiber damage on the inner surface of the pipe after hydrothermal aging for 3000 h by scanning electron microscopy (Fig. 7i). At the same time, a decrease in the concentration of Si–O bonds was detected in the infrared spectra. Ultimately, the multiple damages caused by hydrothermal aging synergistically exacerbated the rapid degradation of the mechanical properties of GFRP pipes.

4. Conclusions

In this project, the thermal aging behavior and aging mechanism of aromatic amine-cured glass fiber reinforced composite tubes used in oilfield environments were investigated. We designed accelerated aging experiments based on the principle of time-temperature equivalence in thermal oxygen and simulated extracted water environments. Thermal aging experiments were carried out at 95 °C for 5000h and 3000h in two media, circulating air and simulated oilfield water, respectively. The differences in the aging behaviors and aging mechanisms of GFRP tubes at different times under the two conditions were analyzed and discussed, and the intrinsic connection between structural evolution and performance decay was explored. Based on the present experimental results, the following main conclusions were obtained.

1) The observation of the apparent morphology and microstructure of the GFRP pipes after ageing under both conditions revealed that the effect of the thermal oxygen environment on the color change and oxidation process of the surface resin was more significant. Uniform nanoscale micropores and a few matrix shrinkage holes were found

in the pipe cross-section after thermal-oxidative ageing, while damage to the glass fiber cross-section was observed. Hydrothermal ageing further causes dissolution of the surface resin and dissolution of the exposed fibers.

2) IR spectra in total reflectance attenuation mode demonstrate a decreasing concentration of C–O–C and C–H bonds in the resin matrix during thermal oxidation and an increasing concentration of ester C═O and C–O bonds in the oxidation products, indicating that the oxidation products are saturated aldehydes, ketones, esters or carboxylic acids. At the same time, the ageing behavior of resin water absorption and glass fiber hydrolysis during hydrothermal ageing was verified by the intensity changes of –OH and Si–O characteristic bands. Furthermore, NMR hydrogen spectroscopy verified the formation of amides, methyl ethers and carboxylic acids in the thermal oxidation products of epoxy resins.
3) Circumferential tensile tests on GFRP pipes show that both thermal ageing methods cause a rapid reduction in the tensile strength of the pipe, with the hydrothermal environment causing more significant damage to the mechanical properties of the GFRP pipe. This is attributed to the physical dissolution of the resin on the surface of the GFRP pipe due to hydrothermal ageing, significant hydrolytic damage to the exposed fibers on the surface, and the combined damage to the resin/fiber interfacial bonding by chloride ions in simulated oilfield water, resulting in a rapid reduction in the overall GFRP properties.

CRediT authorship contribution statement

Dandan Liao: Conceptualization, Data curation, Investigation, Writing – original draft, Writing – review & editing. **Tan Gu:** Funding acquisition. **Jie Liu:** Methodology. **Siwei Chen:** Project administration. **Fei Zhao:** Data curation. **Son Len:** Writing – original draft. **Jingjie Dou:** Data curation. **Xiwen Qian:** Writing – original draft. **Jun Wang:** Investigation, Supervision.

Declaration of competing interest

We declare that we do not have any commercial or associative interest that represents a conflict of interest in connection with the work submitted, and manuscript is approved by all authors for publication. I would like to declare on behalf of my co-authors that the work described was original research that has not been published previously, and not under consideration for publication elsewhere, in whole or in part. All the authors listed have approved the manuscript that is enclosed.

Data availability

The authors do not have permission to share data.

Acknowledgements

The authors also acknowledge the support of China National Petroleum Corporation (CNPC) for the project “Research on Aging Mechanism and Life Prediction of Non-metallic Pipelines”, Project No. Z1H1412.

References

[1] Haris NIN, Hassan MZ, Ilyas RA, Suhot MA, Sapuan SM, Dolah R, Mohammad R, Asyraf MRM. Dynamic mechanical properties of natural fiber reinforced hybrid polymer composites: a review. J Mater Res Technol 2022;19:167–82.
[2] Ogbonna VE, Popoola API, Popoola OM, Adeosun SO. A review on corrosion, mechanical, and electrical properties of glass fiber-reinforced epoxy composites for high-voltage insulator core rod applications: challenges and recommendations. Polym Bull 2022;79:6857–84.
[3] Alabtah FG, Mahdi E, Eliyan FF. The use of fiber reinforced polymeric composites in pipelines: a review. Compos Struct 2021;276:114595.
[4] Budhe S, Banea MD, de Barros S. Composite repair system for corroded metallic pipelines: an overview of recent developments and modelling. J. MAR. SCI. TECH.-JAPAN 2020;25:1308–23.
[5] Morampudi P, Namala KK, Gajjela YK, Barath M, Prudhvi G. Review on glass fiber reinforced polymer composites. Mater Today Proc 2021;43:314–9.
[6] Kumre A, Rana RS, Purohit R. A Review on mechanical property of sisal glass fiber reinforced polymer composites. Mater Today Proc 2017;4:3466–76.
[7] Rafiee R. On the mechanical performance of glass-fibre-reinforced thermosetting-resin pipes: a review. Compos Struct 2016;143:151–64.
[8] Liao D, Huang B, Liu J, Qian X, Zhao F, Wang J. Failure analysis of glass fiber reinforced composite pipe for high pressure sewage transport. Eng Fail Anal 2023;144:106938.
[9] Alabtah FG, Mahdi E, Khraisheh M. External corrosion behavior of steel/GFRP composite pipes in harsh conditions. Materials 2021;14:6501.
[10] Huang S, Fu Q, Yan L, Kasal B. Characterization of interfacial properties between fibre and polymer matrix in composite materials – a critical review. J Mater Res Technol 2021;13:1441–84.
[11] Imielińska K, Guillaumat L. The effect of water immersion ageing on low-velocity impact behaviour of woven aramid–glass fibre/epoxy composites. Compos Sci Technol 2004;64:2271–8.
[12] Manalo A, Maranan G, Sharma S, Karunasena W, Bai Y. Temperature-sensitive mechanical properties of GFRP composites in longitudinal and transverse directions: a comparative study. Compos Struct 2017;173:255–67.
[13] Gu Y, Liu H, Li M, Li Y, Zhang Z. Macro- and micro-interfacial properties of carbon fiber reinforced epoxy resin composite under hygrothermal treatments. J. REINF. PLAST. COMP. 2014;33:369–79.
[14] Ridzuan MJM, Abdul Majid MS, Afendi M, Azduwin K, Amin NAM, Zahri JM, Gibson AG. Moisture absorption and mechanical degradation of hybrid Pennisetum purpureum/glass–epoxy composites. Compos Struct 2016;141:110–6.
[15] Hawileh RA, Abu-Obeidah A, Abdalla JA, Al-Tamimi A. Temperature effect on the mechanical properties of carbon, glass and carbon–glass FRP laminates. CONSTR. BUILD. MATER. 2015;75:342–8.
[16] Hawa A, Abdul Majid MS, Afendi M, Marzuki HFA, Amin NAM, Mat F, Gibson AG. Burst strength and impact behaviour of hydrothermally aged glass fibre/epoxy composite pipes. MATER. DESIGN 2016;89:455–64.
[17] Stocchi A, Pellicano A, Rossi JP, Bernal C, Montemartini P. Physical and water aging of glass fiber-reinforced plastic pipes. COMPOS. INTERFACE. 2006;13:685–97.
[18] Reis JML, Martins FDF, Da Costa Mattos HS. Influence of ageing in the failure pressure of a GFRP pipe used in oil industry. Eng Fail Anal 2017;71:120–30.
[19] Marín L, González EV, Maimí P, Trias D, Camanho PP. Hygrothermal effects on the translaminar fracture toughness of cross-ply carbon/epoxy laminates: failure mechanisms. Compos Sci Technol 2016;122:130–9.
[20] Jiang X, Kolstein H, Bijlaard F, Qiang X. Effects of hygrothermal aging on glass-fibre reinforced polymer laminates and adhesive of FRP composite bridge: moisture diffusion characteristics. Compos Appl Sci Manuf 2014;57:49–58.
[21] Gao Y, Liang X, Bao W, Wu C, Li S, Liu Y, Cai Y. Study on liquids diffusion into and relevant corrosion behaviour of glass fibre reinforced polymer used in high voltage composite insulator. High Volt 2020;5:53–61.
[22] Deniz ME, Karakuzu R. Seawater effect on impact behavior of glass–epoxy composite pipes. Compos B Eng 2012;43:1130–8.
[23] Alawsi G, Aldajah S, Rahmaan SA. Impact of humidity on the durability of E-glass/polymer composites. MATER. DESIGN 2009;30:2506–12.
[24] Yang B, Zhang J, Zhou L, Lu M, Liang W, Wang Z. Effect of fiber surface modification on water absorption and hydrothermal aging behaviors of GF/pCBT composites. Compos B Eng 2015;82:84–91.
[25] Chennareddy R, Tuwair H, Kandil UF, ElGawady M, Reda Taha MM. UV-resistant GFRP composite using carbon nanotubes. CONSTR. BUILD. MATER. 2019;220:679–89.
[26] Delor-Jestin F, Drouin D, Cheval PY, Lacoste J. Thermal and photochemical ageing of epoxy resin – influence of curing agents. Polym Degrad Stabil 2006;91:1247–55.
[27] Zhang X, Wu Y, Wen H, Hu G, Yang Z, Tao J. The influence of oxygen on thermal decomposition characteristics of epoxy resins cured by anhydride. Polym. Degrad. Stabil. 2018;156:125–31.
[28] Fan W, Li JL. The effect of thermal aging on properties of epoxy resin. Adv Mater Res 2012;602–604:798–801.
[29] Fan W, Li J, Zheng Y, Guo D. The effect of reinforced structure on thermo-oxidative stability of polymer-matrix composites. J Ind Text 2016;46:237–55.
[30] Zhang M, Zuo C, Sun B, Gu B. Thermal ageing degradation mechanisms on compressive behavior of 3-D braided composites in experimental and numerical study. Compos Struct 2016;140:180–91.
[31] Jojibabu P, Ram GDJ, Deshpande AP, Bakshi SR. Effect of carbon nano-filler addition on the degradation of epoxy adhesive joints subjected to hygrothermal aging. Polym Degrad Stabil 2017;140:84–94.
[32] Lafariefrenot M. Damage mechanisms induced by cyclic ply-stresses in carbon–epoxy laminates: environmental effects. INT. J. FATIGUE 2006;28:1202–16.
[33] Lafarie-Frenot MC, Rouquié S, Ho NQ, Bellenger V. Comparison of damage development in C/epoxy laminates during isothermal ageing or thermal cycling. Compos Appl Sci Manuf 2006;37:662–71.
[34] Lafarie-Frenot MC, Rouquie S. Influence of oxidative environments on damage in c/epoxy laminates subjected to thermal cycling. Compos Sci Technol 2004;64:1725–35.
[35] Rouquie S, Lafariefrenot M, Cinquin J, Colombaro A. Thermal cycling of carbon/epoxy laminates in neutral and oxidative environments. Compos Sci Technol 2005;65:403–9.

[36] Yang Y, Xian G, Li H, Sui L. Thermal aging of an anhydride-cured epoxy resin. Polym Degrad Stabil 2015;118:111–9.
[37] Wang K, Chen Y, Long H, Baghani M, Rao Y, Peng Y. Hygrothermal aging effects on the mechanical properties of 3D printed composites with different stacking sequence of continuous glass fiber layers. Polym Test 2021;100.
[38] Fiore V, Calabrese L, Miranda R, Badagliacco D, Sanfilippo C, Palamara D, Valenza A, Proverbio E. An experimental investigation on performances recovery of glass fiber reinforced composites exposed to a salt-fog/dry cycle. COMPOS. PART B-ENG. 2023;257.
[39] Chen X, Kong Y, Wang M, Huang X, Huang Y, Lv Y, Li G. Wear and aging behavior of vulcanized natural rubber nanocomposites under high-speed and high-load sliding wear conditions. Wear 2022;498–499:204341.
[40] Zhang M, Sun B, Gu B. Accelerated thermal ageing of epoxy resin and 3-D carbon fiber/epoxy braided composites. Compos Appl Sci Manuf 2016;85:163–71.
[41] Reuscher V, Haag S, Patzelt G, Mayer B. Aging of anhydride-hardened epoxies in lubricants at elevated temperatures. J Appl Polym Sci 2017;134:44877.
[42] Colin X, Mavel A, Marais C, Verdu J. Interaction between cracking and oxidation in organic matrix composites. J Compos Mater 2005;39:1371–89.
[43] Wang P, Ke L, Wu H, Leung CKY. Hygrothermal aging effect on the water diffusion in glass fiber reinforced polymer (GFRP) composite: experimental study and numerical simulation. Compos Sci Technol 2022:230.
[44] Soykok IF, Sayman O, Pasinli A. Effects of hot water aging on failure behavior of mechanically fastened glass fiber/epoxy composite joints. COMPOS. PART B-ENG. 2013;54:59–70.
[45] Liu H, Pei C, Yang J, Yang Z. Influence of long-term thermal aging on the microstructural and tensile properties of all-oxide ceramic matrix composites. Ceram Int 2020;46:13989–96.
[46] Yang Z, Yang J. Investigation of long-term thermal aging-induced damage in oxide/oxide ceramic matrix composites. J Eur Ceram Soc 2020;4:1549–56.
[47] Yang Z, Liu H. Effects of thermal aging on the cyclic thermal shock behavior of oxide/oxide ceramic matrix composites. Mater Sci Eng 2020:769.
[48] Yousef S, Eimontas J, Striūgas N, Subadra SP, Abdelnaby MA. Thermal degradation and pyrolysis kinetic behaviour of glass fibre-reinforced thermoplastic resin by TG-FTIR, Py-GC/MS, linear and nonlinear isoconversional models. J Mater Res Technol 2021;15:5360–74.
[49] Lehuy H, Bellenger V, Verdu J, Paris M. Thermal oxidation of anhydride cured epoxies. 1. mechanistic aspects. Polym Degrad Stabil 1992;35:77–86.
[50] Lin YC, Chen X, Zhang HJ, Wang ZP. Effects of hygrothermal aging on epoxy-based anisotropic conductive film. Mater Lett 2006;60:2958–63.
[51] Chughtai AR, Smith DM, Kumosa LS, Kumosa M. FTIR analysis of non-ceramic composite insulators. IEEE T. DIELECT. EL. IN. 2004;11:585–96.
[52] Lippincott ER, Bunting EN. Infrared studies on polymorphs of silicon dioxide and germanium dioxide. J Res Natl Bur Stand 1958;61:61–70. 1934.
[53] Zhong Y, Cheng M, Zhang X, Hu H, Cao D, Li S. Hygrothermal durability of glass and carbon fiber reinforced composites - a comparative study. Compos Struct 2019;211:134–43.
[54] Scheffler C, Foerster T, Maeder E, Heinrich G, Hempel S, Mechtcherine V. Aging of alkali-resistant glass and basalt fibers in alkaline solutions: evaluation of the failure stress by Weibull distribution function. J Non-Cryst Solids 2009;355:2588–95.
[55] Rybin VA, Utkin AV, Baklanova NI. Alkali resistance, microstructural and mechanical performance of zirconia-coated basalt fibers. CEMENT CONCRETE RES 2013;53:1–8.
[56] Rybin VA, Utkin AV, Baklanova NI. Corrosion of uncoated and oxide-coated basalt fibre in different alkaline media. CORROS. SCI. 2016;102:503–9.
[57] Yang P, Zhou Q, Yuan X, van Kasteren JMN, Wang Y. Highly efficient solvolysis of epoxy resin using poly(ethylene glycol)/NaOH systems. Polym Degrad Stabil 2012;97:1101–6.
[58] Ahmad S, Gupta AP, Sharmin E, Alam M, Pandey SK. Synthesis, characterization and development of high performance siloxane-modified epoxy paints. PROG. ORG. COAT. 2005;54:248–55.
[59] Gottlieb H, Kotlyar V, Nudelman A. NMR chemical shifts of common laboratory solvents as trace impurities. J Org Chem 1997;62:7512–5.
[60] Mendelsy DA, Leterrier Y, Manson JAE, Nairn JA. The influence of internal stresses on the microbond test II: physical aging and adhesion. J Compos Mater 2002;36:1655–76.
[61] Wang XQ, Lau D. Atomistic investigation of GFRP composites under chloride environment. Adv Struct Eng 2021;24:1138–49.
[62] Ma L, Meng L, Wu G, Wang Y, Zhao M, Zhang C, Huang Y. Improving the interfacial properties of carbon fiber-reinforced epoxy composites by grafting of branched polyethyleneimine on carbon fiber surface in supercritical methanol. Compos Sci Technol 2015;114:64–71.